Published in final edited form as:
FASEB J. 2011 December ; 25(12): 4415–4422. doi:10.1096/fj.11-183772.

VCAM-1-targeted magnetic resonance imaging reveals subclinical disease in a mouse model of multiple sclerosis

Sébastien Serres[*], **Silvy Mardiguian**[†], **Sandra J. Campbell**[†], **Martina A. McAteer**[‡], **Asim Akhtar**[‡], **Alexandre Krapitchev**[*], **Robin P. Choudhury**[‡], **Daniel C. Anthony**[†], and **Nicola R. Sibson**[*,1]

[*] Cancer Research UK/Medical Research Council Gray Institute for Radiation Oncology and Biology, Department of Oncology, Churchill Hospital, Oxford, UK

[†] Department of Pharmacology, John Radcliffe Hospital, University of Oxford, Oxford, UK

[‡] Department of Cardiovascular Medicine, John Radcliffe Hospital, University of Oxford, Oxford, UK

Abstract

Diagnosis of multiple sclerosis (MS) currently requires lesion identification by gadolinium (Gd)-enhanced or T_2-weighted magnetic resonance imaging (MRI). However, these methods only identify late-stage pathology associated with blood-brain barrier breakdown. There is a growing belief that more widespread, but currently undetectable, pathology is present in the MS brain. We have previously demonstrated that an anti-VCAM-1 antibody conjugated to microparticles of iron oxide (VCAM-MPIO) enables *in vivo* detection of VCAM-1 by MRI. Here, in an experimental autoimmune encephalomyelitis (EAE) mouse model of MS, we have shown that presymptomatic lesions can be quantified using VCAM-MPIO when they are undetectable by Gd-enhancing MRI. Moreover, in symptomatic animals VCAM-MPIO binding was present in all regions showing Gd-DTPA enhancement and also in areas of no Gd-DTPA enhancement, which were confirmed histologically to be regions of leukocyte infiltration. VCAM-MPIO binding correlated significantly with increasing disability. Negligible MPIO-induced contrast was found in either EAE animals injected with an equivalent nontargeted contrast agent (IgG-MPIO) or in control animals injected with the VCAM-MPIO. These findings describe a highly sensitive molecular imaging tool that may enable detection of currently invisible pathology in MS, thus accelerating diagnosis, guiding treatment, and enabling quantitative disease assessment.

The clinicoradiological paradox in multiple sclerosis (MS) refers to the poor association between clinical findings and radiological extent of lesion load (1). The use of MRI as an outcome measure in clinical trials, or a prognosticator in the assessment of disease evolution, assumes a close relationship between the number of MRI-detectable abnormalities and clinical status. Yet, evidence suggests that conventional MRI does not accurately report the extent of pathology. For example, we have shown that both axonal damage and endothelial adhesion molecule expression are ongoing in experimental lesions that are no longer detectable using MRI (2, 3). This disparity between radiological measures and disease severity also presents problems for the assessment of therapeutic efficacy. For example, alemtuzumab, a humanized monoclonal antibody that targets CD52 on lymphocytes and monocytes, has clinical efficacy in patients with early relapsing-remitting

[1]Correspondence: Radiobiology Research Institute, Churchill Hospital, Oxford, OX3 7LJ, UK. nicola.sibson@oncology.ox.ac.uk.

This article includes supplemental data. Please visit http://www.fasebj.org to obtain this information.

Europe PMC Funders Author Manuscripts

MS, yet the effect of this therapy on MRI indexes is less marked (4). The most commonly used imaging marker for MS is the presence of Gd-enhancing or T_2-hyperintense lesions in the central nervous system, as defined in the revised McDonald criteria (5). However, both Gd accumulation and T_2 hyperintensity reflect relatively advanced downstream pathology with blood-brain barrier (BBB) breakdown and edema accumulation. There is a growing belief that there is more widespread pathology in the MS brain than these imaging methods suggest, with more generalized vascular activation (6) and that it may be this undetectable extralesional disease that underlies clinical progression. It is clear, therefore, that there is a need for diagnostic tools that enable more accurate and specific measures of disease activity.

We have recently shown that targeted MRI contrast agents, which reversibly adhere to specific molecules, can reveal disease at a time when conventional images obtained are normal (3, 7,–,9). Endothelial vascular cell adhesion molecules are key mediators of leukocyte recruitment. Vascular cell adhesion molecule-1 (VCAM-1) has been shown to be important in the development of experimental autoimmune encephalomyelitis (EAE) and MS, mediating both leukocyte movement across the BBB and their retention within the parenchyma during a relapse (10). Selective blockade of the interaction between VCAM-1 and its ligand, integrin $\alpha_4 \beta_1$ (VLA-4), on leukocytes has been shown to abolish leukocyte recruitment and the associated neurological deficit in EAE models (11). Similarly, selective VLA-4 inhibitors reduce the number of MRI-detectable lesions in MS (12). We have previously developed a targeted MRI-detectable contrast agent, consisting of microparticles of iron oxide (MPIO; 1 μm) conjugated to anti-VCAM-1 antibody (VCAM-MPIO), which binds to activated endothelium *in vivo* (7). Thus, the aim of the current study was to determine the sensitivity of VCAM-MPIO for early and more accurate disease detection in a well-established and clinically relevant EAE model of MS.

MATERIALS AND METHODS

EAE model

Female SJL mice (8 to 12 wk old, 25 g; Harlan, Bicester, UK) were injected subcutaneously at the tail-base with either 50 μl complete Freud's adjuvant (CFA; Sigma-Aldrich, Gillingham, UK; control; n=3) or 25 μg of proteolipid protein (PLP; Activotec, Comberton, UK) in 50 μl of CFA (EAE; n=19). All animals were also injected intravenously with 200 ng of pertussis toxin (Sigma-Aldrich) in 0.2 ml of phosphate buffered saline at both d 0 and 2. Animals were weighed and assessed daily for clinical signs according to the following guidelines: 0, healthy; 1, slight loss of tail tone; 2, complete loss of tail; 3, weakness in the limbs; and 4, paralysis. All experiments were performed with UK Home Office approval.

VCAM-MPIO synthesis

Purified monoclonal rat anti-mouse antibodies to VCAM-1 (clone M/K2; Cambridge Bioscience, Cambridge, UK) or control IgG-1 (clone Lo-DNP-1; Serotec, Kidlington, UK) were conjugated to myOne tosylactivated MPIO (1 μm diameter; iron content 26%; Invitrogen, Carlsbad, CA, USA) with p-toluenesulfonyl (tosyl)-reactive surface groups (Invitrogen) as described previously (7).

Experimental protocol

EAE animals were injected intravenously *via* a tail vein with 100 μl VCAM-MPIO (4 mg Fe/kg body weight) at d 8 (n=4), 12 (n=4), or 15 (n=6) after immunization and underwent MRI from 1 h postinjection. Two further groups of EAE animals at d 8 (n=2) and 12 (n=3) were injected intravenously with 100 μl IgG-MPIO, as a nontargeted control, and underwent MRI from 1 h postinjection. Control (CFA only) animals were injected with 100 μl VCAM-MPIO at d 12 and imaged as above (n=3). The mice were anesthetized with 1–2% isoflurane

Europe PMC Funders Author Manuscripts

in 70% N_2O/30% O_2 and positioned in a quadrature birdcage coil (2.6 cm inner diameter; Rapid MR International, Würzburg, Germany). ECG was monitored throughout and body temperature maintained at ~37°C. MRI data were acquired in a 7-T horizontal-bore magnet with a Varian Inova spectrometer (Varian, Washington, DC, USA).

MRI

For detection of VCAM-MPIO, a T_2*-weighted 3-D gradient echo data set was acquired as follows: flip angle, 31°; repetition time, 50 ms; echo time, 5 ms; field of view, 11.2 × 22.5 × 22.5 mm; matrix size, 96 × 192 × 256; 2 averages; total acquisition time, ~40 min. The midpoint of acquisition was 1.5 ± 0.25 h after MPIO injection. Data were zero-filled to 128 × 256 × 256 and reconstructed offline, giving a final isotropic resolution of 88 μm. Subsequently, a set of 7 T_1-weighted images (coronal, 1 mm thick; in-plane resolution *ca.* 175 μm; acquisition time *ca.* 4 min) were acquired using a spin-echo sequence (TR = 500 ms; TE = 13 ms) both before and 5 min after intravenous injection of 30 μl Gd-DTPA (Omniscan; GE Healthcare, Little Chalfont, UK) to identify BBB permeability. This dose is equivalent to 1.2 ml/kg, which is double the human high dose often used for the detection of MS lesions (0.6 ml/kg; ref. 13).

MRI data analysis

The T_2*-weighted data set was converted into tiff images, manually masked to exclude extracerebral structures, and converted to 8-bit grayscale in Adobe Photoshop (Adobe Systems, Uxbridge, UK). The images were thresholded at a consistent level in the gray channel, such that any pixels of signal intensity >3 sd below the mean intensity of normal brain were set to 0 (black) and all others were set to 1 (white). The absolute level of thresholding varied between data sets according to variations in signal-to-noise ratio, but interanimal consistency of thresholding was assessed through repeat analysis and multiple independent operators. Signals arising from ventricles or sinuses were excluded by comparison to a naive animal imaged with no contrast agent, in which these structures appear hypointense naturally. The masked and thresholded images were subsequently imported into ImagePro (Media Cybernetics, Marlowe, UK) and stacked into a single sequence. MPIO binding, defined as all pixels with signal levels of 0, was quantified in 256 consecutive brain slices for each animal. Analysis was performed blind to the origin of the dataset. Segmented images were reconstructed using the 3D Constructor plug-in to visualize the spatial distribution of MPIO binding, with low-signal areas assigned to the red channel and the anatomical image to the green channel. Voxel volumes were summed and expressed as raw volumes in microliters with no further surface rendering or smoothing effects, beyond the 0-filling applied during data processing.

To determine the correspondence between $VCAM^+$ lesions and Gd-DTPA enhancement, each of the 7 T_1-weighted images and the corresponding T_2*-weighted images was positioned on grids of standard size. Within each square on the grid, the number of VCAM-$MPIO^+$ lesions (evident as discrete focal hypointensities) were counted and classified as either Gd-$DTPA^+$ (*i.e.*, within a region of Gd-DTPA contrast enhancement) or Gd-$DTPA^-$. Values were calculated as the mean number of lesions ($VCAM^+/Gd^+$; $VCAM^+/Gd^-$) per single slice. The number of squares showing gadolinium-enhancement that did not encompass any T_2* hypointensities was also counted. Regions of Gd-DTPA enhancement were identified as regions of visibly increased signal intensity both on the original post-Gd $T1$-weighted images and on the difference (post-Gd-DTPA minus pre-Gd-DTPA) images.

Immunohistochemistry: mouse tissue

Day-15 EAE animals were split into 2 groups (n=3/group) for immunohistochemistry. Animals in the first group were transcardially perfused under terminal anesthesia with 0.9%

Europe PMC Funders Author Manuscripts

heparinized saline followed by 200 ml periodate lysine paraformaldehyde. The brains were postfixed, cryoprotected, embedded, and frozen in isopentane at −40°. Then, 10-μm-thick coronal brain sections, corresponding to the locations of the 7 T_1-weighted imaging slices, were stained for macrophages using the F4/80 antibody (Serotec) and appropriate biotinylated secondary reagents with standard ABC amplification (Vector Laboratories, Peterborough, UK). Immunoreactivity was revealed with DAB to produce a brown insoluble precipitate. For the second group of d-15 EAE animals, the brains were removed following perfusion with heparinized saline only and frozen in Tissue-Tek (Sakura Finetek, Torrance, CA, USA) in isopentane over dry ice. Frozen 10-μm cryosections were fixed for 20 min in 100% ethanol before immunostaining with the M/K2 hybridoma for mouse VCAM-1 (1 μg/ml) using standard ABC amplification procedures.

Immunohistochemistry: human tissue

MS (n=5) and control (n=4) brain tissue was provided by the Thomas Willis Oxford Brain Collection (University of Oxford) with full ethical approval. Immunohistochemistry was carried out with anti-VCAM-1 (ATCCHB10519), using ABC amplification and DAB development.

Statistics

Statistical analysis was performed using SPSS (SPSS Inc., Chicago, IL, USA). ANOVA was used to identify overall significant differences in the measured volumes of hypointensity, followed by pairwise t tests to identify specific differences between the groups. The relationship between clinical scores and volumes of VCAM-MPIO hypointensity was tested by a bivariate correlation analysis including calculation of Spearman's ρ (r) after rank transformation of the parametric volumes. Data are expressed as means ± se.

RESULTS

The earliest clinical signs (reduced tail tone; score 1) occurred 9–10 d after immunization and became progressively worse thereafter. The disease was most severe at d 12, with complete hindlimb paralysis (score 4), followed by a gradual remission from d 15 onward (**Fig. 1*A***). Weight loss was also evident from d 9, reaching a maximum loss (20% of original body weight) at the peak of disease severity.

In vivo MRI detects VCAM-MPIO bound to brain endothelium in EAE mice

VCAM-MPIO caused a marked MRI contrast effect, evident as focal hypointense areas on T_2*-weighted images. VCAM-MPIO binding was observed from the earliest time point studied, d 8 (Figs. 1*B* and 2), despite a complete lack of clinical signs (score 0). As the disease progressed and neurological deficits became manifest, the degree of VCAM-MPIO binding increased markedly (Figs. 1*C* and 2). We detected little or no MPIO retention at d 12 in either EAE mice administered the control contrast agent (IgG-MPIO) or CFA animals injected with VCAM-MPIO (Figs. 1*B* and 2). To confirm this lack of nontargeted contrast effects, 2 additional EAE animals were injected with IgG-MPIO at d 8 and showed similarly low levels of background contrast (0.85 and 1.07, compared with 0.86±0.13 μl at d 12). Quantitatively, VCAM-MPIO binding in EAE animals was significantly greater than that measured in both control CFA mice and EAE mice administered with IgG-MPIO from as early as d 8 after induction when clinical score was 0 (P<0.05; Fig. 1*B*), indicating the detection of EAE lesions in asymptomatic animals. VCAM-MPIO binding increased significantly between d 8 and 15 (P<0.05; Fig. 1*C*).

The anatomical distribution of contrast effect changed with disease progression. At d 8 (presymptomatic), VCAM-MPIO binding was detected in EAE mice in the caudal half of

Europe PMC Funders Author Manuscripts

the forebrain and the hindbrain. Subsequently, at d 12 and 15, VCAM-1 expression became evident throughout the forebrain (Fig. 2). Quantitation of VCAM-MPIO binding in single MRI slices from 3 different areas of the brain, forebrain, midbrain, and hindbrain, showed that VCAM-MPIO binding increased significantly in the forebrain and hindbrain slices over time ($P<0.05$; Fig. 1*D*). Correlation analysis following rank transformation of the hypointense volume data demonstrated a positive correlation between the volume of MPIO binding across the whole brain and clinical score ($P<0.0001$; $r=0.89$; Fig. 1*E*).

Comparison with clinically used Gd-DTPA enhancement

No Gd-DTPA enhancement was found on T_1-weighted images from presymptomatic (d 8) EAE animals, indicating a lack of BBB breakdown, despite clear VCAM-MPIO binding. At later time points, some Gd-DTPA-enhancing lesions were evident, yet a substantial number of lesions at d 12 and 15 were notably Gd-DTPA$^-$ but VCAM-MPIO$^+$ (Figs. 1*F* and 3*A*, *B*). Notably, no lesions in EAE animals showing BBB breakdown (Gd-DTPA$^+$) were VCAM-MPIO$^-$. It is possible that, even with the spin-echo sequence used to acquire T_1-weighted data, some T_2 contrast effects of the bound VCAM-MPIO could remain and confound the detection of T_1 contrast enhancement owing to Gd accumulation. However, we found no evidence of hypointensities on the pre-Gd T_1-weighted images even at d 15 (Supplemental Data), and, indeed, it is unlikely that any residual negative T_2 contrast effect would exactly match the positive T_1 contrast effect in magnitude, location and spatial extent. Moreover, even in our post-VCAM-MPIO T_2-weighted images, which were acquired with a longer TE (*i.e.*, greater $T2$ weighting), T_2 contrast effects were only observed at later time points (d 12–15) when VCAM-MPIO binding was substantial, and then only infrequently (Supplemental Data). It is also of note that no evidence of hyperintense lesions on the T_2-weighted images, an alternative clinically used marker for MS lesions, was found at any time point (Supplemental Data).

The number of VCAM-MPIO$^+$/Gd-DTPA$^-$ lesions was significantly higher ($P<0.05$) than VCAM-MPIO$^+$/Gd-DTPA$^+$ lesions at all time points (Fig. 1*F*), indicating that VCAM-1 expression in EAE animals precedes BBB breakdown. In EAE animals injected with VCAM-MPIO, no Gd-DTPA$^+$ lesions were VCAM-MPIO$^-$. In EAE animals injected with IgG-MPIO, some Gd-DTPA$^+$/MPIO$^-$ lesions were evident, suggesting that there is no retention of MPIO across a compromised BBB, likely owing to the larger size of the MPIO compared with Gd-DTPA. Further, the low level of MPIO contrast in both EAE animals injected with IgG-MPIO and CFA animals injected with VCAM-MPIO confirms that there is very little nonspecific binding of the MPIO (Fig. 1*F*).

Immunohistochemical analysis of EAE and MS tissue

VCAM-1 expression in EAE mice was confirmed by immunohistochemistry (Fig. 3*C*–*F*), showing a distribution that was limited to brain vascular endothelium without evidence of extravasation. We found no evidence of constitutive VCAM-1 expression in the brain (Fig. 3*E*), in accord with the VCAM-MPIO MRI data showing little retention of the VCAM-MPIO in control animals. The regions of T_2* hypointensity and Gd-DTPA enhancement observed by MRI correlated spatially with areas of macrophage recruitment/microglial activation, confirmed immunohistochemically (Fig. 3*C, D*).

To confirm the presence of VCAM-1 in human MS tissue, we undertook immunohistochemistry on *post mortem* brain tissue from MS patients, encompassing all types of MS (primary progressive, secondary progressive and relapsing remitting). VCAM-1 expression was observed in all cases in association with the active border of plaques and adjacent normal appearing gray and white matter (Fig. 4). No immunoreactivity was observed in control brains.

Europe PMC Funders Author Manuscripts

DISCUSSION

In this study, we have reported the application of a molecular imaging probe that facilitates the early identification of disease in a murine model of MS *in vivo* by MRI. The anti-VCAM-1-based contrast agent enables detection of EAE before clinical signs are evident and reveals pathology previously inaccessible to conventional, clinically used MRI techniques. The results of this study raise the potential for both earlier diagnosis of MS and more sensitive monitoring of disease progression, which may generate significant clinical advantage. It is generally accepted that current clinical practice, both radiological and neurological, does not describe the full disease burden in MS patients. There is growing speculation that more widespread, extralesional inflammatory pathology in both MS and EAE (6, 14) that is not revealed by either Gd-enhanced or T_2-weighted MRI (6) may be the true indicator of disease progression and severity. In this case, our VCAM-1-targeted approach would provide a very sensitive measure of disease activity and, thus, has considerable potential as a biomarker of therapeutic efficacy in both preclinical/clinical trials and in clinical practice. Indeed, a lack of suitable biomakers in MS is one of the reasons for the protracted timescales for the pharmaceutical pipeline in this disease. Similarly, a lack of sensitive indexes of therapeutic efficacy hampers the early identification of nonresponder patients (15), which is crucial to ensure that the appropriate therapeutic is selected at an early stage. Clinical trials in patients with MS have demonstrated clear clinical benefits arising from inhibition of the interaction between VCAM-1 and its ligand VLA-4 (12). The ability, therefore, to image VCAM-1 expression, in conjunction with existing diagnostic approaches, may offer clinically important opportunities not only for disease diagnosis and monitoring but also for targeting therapy and monitoring response to treatment.

Detection of acute VCAM-1 expression facilitates early diagnosis

The use of the VCAM-1-targeted MPIO revealed the presence of VCAM-1 expression, which, hitherto, could only be observed *ex vivo*. In this way, molecular imaging with targeted MRI-visible contrast confers the ability to perform "*in vivo* biopsies," with the potential advantage of serially monitoring individual lesions over an extended time course. The diagnostic imaging window with current conventional MRI techniques is restricted to periods when gross anatomical changes produce perturbations in the proton signal. High-dose Gd-DTPA, as used here, is often used for lesion detection in MS, but it remains a passive agent that requires a loss of BBB integrity.

EAE lesions develop behind an intact BBB, and thus it should come as no surprise that VCAM-1 expression occurs in advance of BBB breakdown. The ability to overcome the apparent immune privilege of the central nervous system by the generation of EAE was the first demonstration that leukocytes were able to cross an intact BBB. Previous studies have suggested that increased BBB permeability precedes the occurrence of histological lesions (16), but our investigations reveal a clear temporal and spatial mismatch between Gd-DTPA accumulation in the brain and the appearance of VCAM-1$^+$ vessels, surrounded by cuffs of leukocytes, before breakdown of the BBB that is detectable by Gd-enhanced MRI. This is in accord with recent reports that axonal damage begins well ahead of the appearance of motor symptoms in MS and highlights the importance of early detection strategies (17).

Specificity of VCAM-MPIO

One of the major strengths of our VCAM-MPIO agent is the very short (<5 min) half-life of micrometer-sized iron oxide particles in the circulation (18, 19). As a result, at the time point that imaging is started (1 h post-VCAM-MPIO administration), negligible contrast agent, and associated contrast effects, remain in the blood. This is particularly evident in the control groups where little evidence of nonspecific hypointensity in the brain is seen, either

Europe PMC Funders Author Manuscripts

in VCAM-MPIO-injected CFA-only mice or IgG-MPIO-injected EAE mice. These data also indicate the specificity of the VCAM-1 targeted MPIO for its intended target, as we have previously demonstrated through blocking experiments (7).

Although some have suggested that there is constitutive expression of VCAM-1 in the brain (20), as in the bone marrow and lymphoid tissue, we have found no evidence of this either in mice, using both RT-PCR and immunohistochemistry, or control human tissue. Furthermore, both the present study and our previous work (7) would support a lack of constitutive expression, since no retention of the VCAM-MPIO is observed in either naive or control animals. It seems probable that the pattern of adhesion molecule expression will change during the progression of MS, and other adhesion molecules, such as ALCAM (21) or the selectins (3), have been shown to be particularly elevated in the chronic-stages of MS and EAE. Similarly, previous work by Sipkins *et al.* (22) demonstrated increased ICAM-1 expression in EAE using antibody-conjugated paramagnetic liposomes and *ex vivo* high-resolution MRI. Although, with respect to ICAM-1, we have found that following a focal unilateral injection of cytokines into the brain ICAM-1 expression is considerably more widespread than either VCAM-1 or E-/P-selectin (unpublished results), which may prove a confound when looking for a spatially specific biomarker of inflammatory lesions. Nevertheless, it is likely that the ability to place other specific antiadhesion targeting ligands on the MPIO platform will further aid selection of appropriate therapy across disease pathogenesis.

Temporal progression of VCAM-1 expression in EAE

Over time, the volume of hypointensity induced by VCAM-MPIO binding increased throughout the brain and showed a positive correlation with both time and clinical score. These findings demonstrate the potential of molecularly targeted MRI methods for detecting specific molecular signatures in a robust and reproducible manner throughout a disease time course. Such information has not previously been accessible *in vivo*. Interestingly, the most marked increases in VCAM-1 expression were evident in the hindbrain. It is not clear why the hindbrain, which includes the cerebellum, should be more susceptible to EAE, although it is known that some forms of this disease target certain structures more than others and that this is often strain-dependent (17). The localization of inflammatory foci within the cerebellum is correlated with severe clinical outcomes in MS, and EAE studies have revealed distinct clinical outcomes correlated with the capacity of the animal to produce IFN-γ (23). Microinjection of IFN-γ along the neuraxis has been shown to provoke distinct patterns of inflammation, which suggests regional variations in the local regulatory environment that could contribute to site-specific immune regulation and may affect the distribution of MS plaques (24).

VCAM-1 expression in MS

VCAM-1 appears to be a particularly good target for the early detection of MS-like lesions, and our immunohistochemical analysis of human tissue supports this. Although marked increases in soluble VCAM-1 have been reported (25), there has been considerable controversy as to the cellular localization of vascular VCAM-1 in MS, with reports of both positive (20, 26) and negative (6) endothelial VCAM-1 immunoreactivity in MS plaques. These apparent discrepancies have generated some debate over the role of adhesion molecules in leukocyte trafficking in MS and have led to confusion about the mode of action of the anti-VLA-4 therapeutic, tysabri, in MS. For this reason, we investigated the expression of VCAM-1 on endothelial cells in MS tissue, not only within the lesions themselves, but also in surrounding normal-appearing tissue. It was evident that expression of VCAM-1 was up-regulated on vessels, but more obviously in surrounding normal-appearing tissue than the plaques themselves. This finding is in accord with the recent report

Europe PMC Funders Author Manuscripts

of Allavena *et al.* (20) in which VCAM immunoreactivity was maximal in patients with acute active plaques but demonstrated a diffuse, rather than focal, distribution. These observations support a hypothesis of widespread vascular activation during acute active disease in MS and suggest that the VCAM-targeted MRI approach may be highly sensitive to this more widespread extralesional activity in otherwise normal-appearing tissue.

Translation to the clinic

While the current findings are encouraging, a number of hurdles must be overcome before such agents can be used clinically; perhaps the most important will be the development of fully biodegradable MPIO and anti-human analogues of the targeting antibodies, together with full toxicological testing of the humanized and biodegradable agent. Nevertheless, to date we have observed no toxicological effects of the VCAM-MPIO used in any mice, which includes recovery following the initial MRI session and reimaging 3 d later with an additional VCAM-MPIO dose.

In conclusion, we have developed a molecular imaging approach that facilitates the early identification of disease in a murine model of MS *in vivo* by MRI. This is the first demonstration that a targeted MRI contrast agent enables subclinical detection of neurological disease in a clinically relevant model. These findings suggest that VCAM-MPIO may be a sensitive diagnostic tool for the detection of MS pathology and may enable more accurate determination of disease burden than either the clinical scoring system or current imaging methods for MS diagnosis. While it is not possible to use this approach in MS patients before the initial onset of neurological symptoms, we propose that it may accelerate diagnosis and remove the current diagnostic requirement for MRI-detectable lesions disseminated in time or space. Moreover, the sensitivity of this technique suggests that subclinical disease may be detectable in patients with MS and, consequently, could enable prediction of relapse and more precise assessment of treatment, as well as enabling targeted treatment for patients with elevated VCAM-1. The MRI readout provides a readily quantifiable measure of lesion burden, which is not currently available and could be standardized across clinical centers with relative ease. Thus, this new VCAM-targeted molecular MRI approach has the potential to address the major limitations inherent in current clinical management of MS; ambiguity in diagnostic indices and radiological-neurological disparity.

Supplementary Material

Refer to Web version on PubMed Central for supplementary material.

Acknowledgments

The authors thank Dr. Andrew Lowe for technical assistance.

This work was supported by the Medical Research Council, research grant G0401438 (to N.S.) and by The Wellcome Trust (to R.C.). S.J.C., R.P.C., D.C.A., and N.R.S. are cofounders of a University of Oxford spinoff company, Oxford Contrast.

REFERENCES

1. Barkhof F. The clinico-radiological paradox in multiple sclerosis revisited. Curr. Opin. Neurol. 2002; 15:239–245. CrossRefMedline. [PubMed: 12045719]
2. Newman TA, Woolley ST, Hughes PM, Sibson NR, Anthony DC, Perry VH. T-cell- and macrophage-mediated axon damage in the absence of a CNS-specific immune response: involvement of metalloproteinases. Brain. 2001; 124:2203–2214. [PubMed: 11673322]

Europe PMC Funders Author Manuscripts

3. Serres S, Anthony DC, Jiang Y, Broom KA, Campbell SJ, Tyler DJ, van Kasteren SI, Davis BG, Sibson NR. Systemic inflammatory response reactivates immune-mediated lesions in rat brain. J. Neurosci. 2009; 29:4820–4828. [PubMed: 19369550]
4. Coles AJ, Compston DA, Selmaj KW, Lake SL, Moran S, Margolin DH, Norris K, Tandon PK. Alemtuzumab vs. interferon beta-1a in early multiple sclerosis. N. Engl. J. Med. 2008; 359:1786–1801. [PubMed: 18946064]
5. Polman CH, Reingold SC, Edan G, Filippi M, Hartung HP, Kappos L, Lublin FD, Metz LM, McFarland HF, O'Connor PW, Sandberg-Wollheim M, Thompson AJ, Weinshenker BG, Wolinsky JS. Diagnostic criteria for multiple sclerosis: 2005 revisions to the "McDonald criteria. Ann. Neurol. 2005; 58:840–846. [PubMed: 16283615]
6. Peterson JW, Bo L, Mork S, Chang A, Ransohoff RM, Trapp BD. VCAM-1-positive microglia target oligodendrocytes at the border of multiple sclerosis lesions. J. Neuropathol. Exp. Neurol. 2002; 61:539–546. [PubMed: 12071637]
7. McAteer MA, Sibson NR, von Zur Muhlen C. Schneider JE, Lowe AS, Warrick N, Channon KM, Anthony DC, Choudhury RP. In vivo magnetic resonance imaging of acute brain inflammation using microparticles of iron oxide. Nat. Med. 2007; 13:1253–1258. [PubMed: 17891147]
8. Van Kasteren SI, Campbell SJ, Serres S, Anthony DC, Sibson NR, Davis BG. Glyconanoparticles allow pre-symptomatic in vivo imaging of brain disease. Proc. Natl. Acad. Sci. U. S. A. 2009; 106:18–23. [PubMed: 19106304]
9. Von Zur, Muhlen C.; Sibson, NR.; Peter, K.; Campbell, SJ.; Wilainam, P.; Grau, GE.; Bode, C.; Choudhury, RP.; Anthony, DC. A contrast agent recognizing activated platelets reveals murine cerebral malaria pathology undetectable by conventional MRI. J. Clin. Invest. 2008; 118:1198–1207. [PubMed: 18274670]
10. Graesser D, Mahooti S, Madri JA. Distinct roles for matrix metalloproteinase-2 and alpha4 integrin in autoimmune T cell extravasation and residency in brain parenchyma during experimental autoimmune encephalomyelitis. J. Neuroimmunol. 2000; 109:121–131. [PubMed: 10996214]
11. Yednock TA, Cannon C, Fritz LC, Sanchez-Madrid F, Steinman L, Karin N. Prevention of experimental autoimmune encephalomyelitis by antibodies against alpha 4 beta 1 integrin. Nature. 1992; 356:63–66. [PubMed: 1538783]
12. Polman CH, O'Connor PW, Havrdova E, Hutchinson M, Kappos L, Miller DH, Phillips JT, Lublin FD, Giovannoni G, Wajgt A, Toal M, Lynn F, Panzara MA, Sandrock AW. A randomized, placebo-controlled trial of natalizumab for relapsing multiple sclerosis. N. Engl. J. Med. 2006; 354:899–910. [PubMed: 16510744]
13. Giacomini PS, Levesque IR, Ribeiro L, Narayanan S, Francis SJ, Pike GB, Arnold DL. Measuring demyelination and remyelination in acute multiple sclerosis lesion voxels. Arch. Neurol. 2009; 66:375–381. [PubMed: 19273757]
14. Howell OW, Rundle JL, Garg A, Komada M, Brophy PJ, Reynolds R. Activated microglia mediate axoglial disruption that contributes to axonal injury in multiple sclerosis. J. Neuropathol. Exp. Neurol. 2010; 69:1017–1033. [PubMed: 20838243]
15. Tedeschi G, Gallo A. Multiple sclerosis patients and immunomodulation therapies: the potential role of new MRI techniques to assess responders versus non-responders. Neurol. Sci. 2005; 26(Suppl. 4):S209–S212. [PubMed: 16388360]
16. Juhler M, Barry DI, Offner H, Konat G, Klinken L, Paulson OB. Blood-brain and blood-spinal cord barrier permeability during the course of experimental allergic encephalomyelitis in the rat. Brain Res. 1984; 302:347–355. [PubMed: 6610460]
17. Ayers MM, Hazelwood LJ, Catmull DV, Wang D, McKormack Q, Bernard CC, Orian JM. Early glial responses in murine models of multiple sclerosis. Neurochem. Int. 2004; 45:409–419. [PubMed: 15145555]
18. Tang KS, Hann B, Shapiro EM. On the use of micron-sized iron oxide particles (MPIOS) to label resting monocytes in bone marrow. Mol. Imaging Biol. 2010 [E-pub ahead of print]. doi: 10.1007/s11307-010-0437-3.
19. Yang Y, Yang Y, Yanasak N, Schumacher A, Hu TC. Temporal and noninvasive monitoring of inflammatory-cell infiltration to myocardial infarction sites using micrometer-sized iron oxide particles. Magn. Reson. Med. 2010; 63:33–40. [PubMed: 19953508]

Europe PMC Funders Author Manuscripts

20. Allavena R, Noy S, Andrews M, Pullen N. CNS elevation of vascular and not mucosal addressin cell adhesion molecules in patients with multiple sclerosis. Am. J. Pathol. 2010; 176:556–562. [PubMed: 20035048]

21. Cayrol R, Wosik K, Berard JL, Dodelet-Devillers A, Ifergan I, Kebir H, Haqqani AS, Kreymborg K, Krug S, Moumdjian R, Bouthillier A, Becher B, Arbour N, David S, Stanimirovic D, Prat A. Activated leukocyte cell adhesion molecule promotes leukocyte trafficking into the central nervous system. Nat. Immunol. 2008; 9:137–145. Medline. [PubMed: 18157132]

22. Sipkins DA, Gijbels K, Tropper FD, Bednarski M, Li KC, Steinman L. ICAM-1 expression in autoimmune encephalitis visualized using magnetic resonance imaging. J. Neuroimmunol. 2000; 104:1–9. CrossRefMedline. [PubMed: 10683508]

23. Lees JR, Golumbek PT, Sim J, Dorsey D, Russell JH. Regional CNS responses to IFN-gamma determine lesion localization patterns during EAE pathogenesis. J. Exp. Med. 2008; 205:2633–2642. [PubMed: 18852291]

24. Phillips LM, Lampson LA. Site-specific control of T cell traffic in the brain: T cell entry to brainstem vs. hippocampus after local injection of IFN-gamma. J. Neuroimmunol. 1999; 96:218–227. [PubMed: 10337920]

25. Hellings N, Gelin G, Medaer R, Bruckers L, Palmers Y, Raus J, Stinissen P. Longitudinal study of antimyelin T-cell reactivity in relapsing-remitting multiple sclerosis: association with clinical and MRI activity. J. Neuroimmunol. 2002; 126:143–160. [PubMed: 12020966]

26. Cannella B, Raine CS. The adhesion molecule and cytokine profile of multiple sclerosis lesions. Ann. Neurol. 1995; 37:424–435. [PubMed: 7536402]

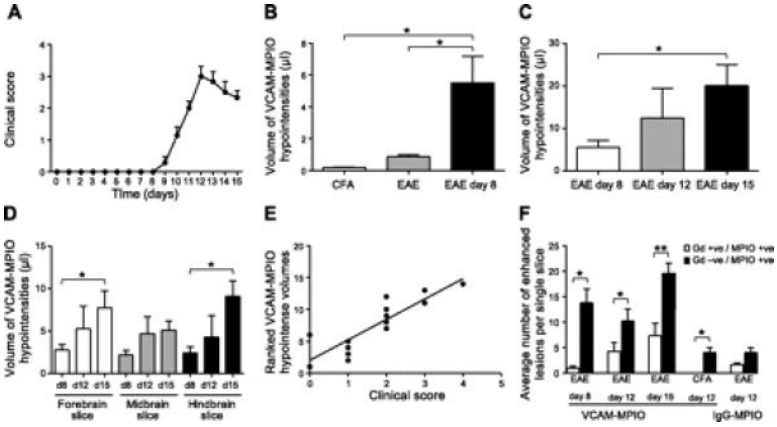

fig 1.

Europe PMC Funders Author Manuscripts

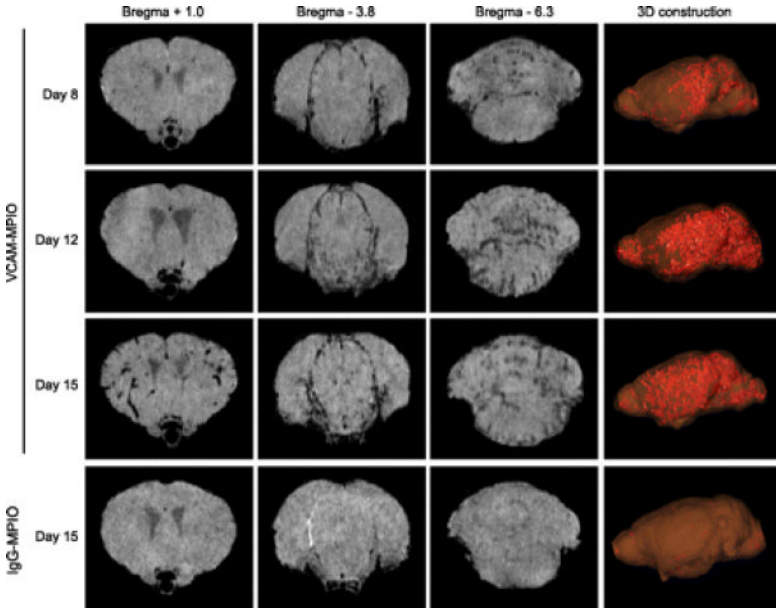

fig 2.

Europe PMC Funders Author Manuscripts

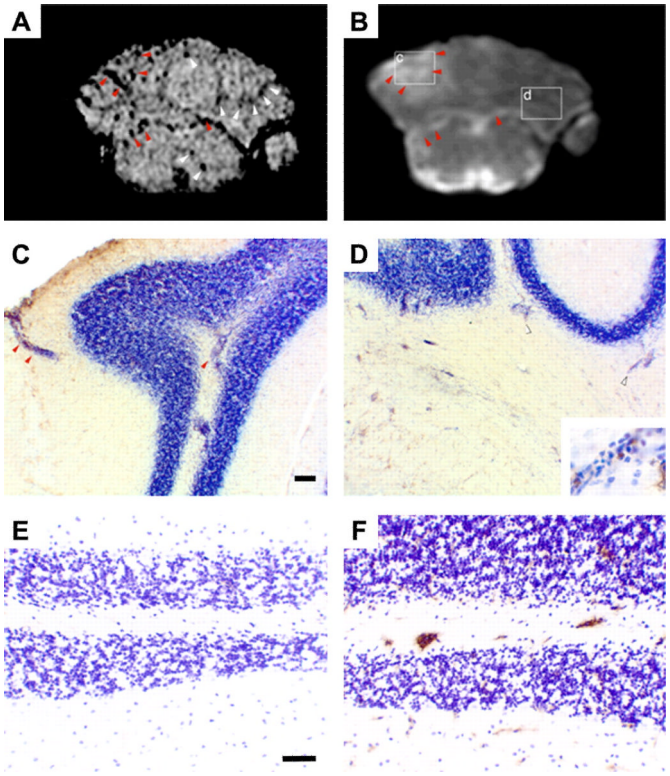

fig 3.

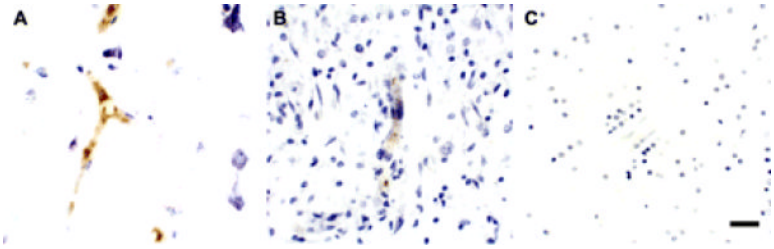

fig 4.